

# ENHANCING LARGE-SCALE STRUCTURE DIAGNOSTICS THROUGH UAV-BASED DATA AND NEURAL NETWORK ANALYSIS

**L.M. Lobanov, I.L. Shkurat, D.I. Stelmakh, O.P. Shutkevych, V.V. Savitsky**

E.O. Paton Electric Welding Institute of the NASU  
11 Kazymyr Malevych Str., 03150, Kyiv, Ukraine

## ABSTRACT

The article presents an approach to remote diagnostics of damage to large-scale engineering structures using unmanned aerial vehicles (UAVs) and convolutional neural networks. The study was conducted to automate the process of detecting structural defects in the Kyiv TV tower. The research methodology involved the collection and preprocessing of 14187 images and the development of a modified architecture of the U-Net neural network for damage segmentation. An experimental study of different architectural settings of the model demonstrated the effectiveness of the proposed modifications, which allowed reducing the error of defect detection by 3–5 % compared to the baseline models. It was found that the optimal number of training iterations is 15–20 epochs. The developed model demonstrated the ability to detect damage that may be missed by the operator, which confirms the potential of automated diagnostic systems based on artificial intelligence. The study provides new prospects for improving the efficiency of monitoring infrastructure facilities, especially under conditions of limited access or increased risks to personnel.

**KEYWORDS:** remote diagnostics, defects, artificial intelligence, neural networks, image segmentation, UAVs

## INTRODUCTION

Systematic monitoring of the technical condition of large-scale facilities is important for assessing their structural integrity. Over time, structures undergo changes caused by corrosion, ageing of materials, loads and external factors.

For the safe and continuous operation of large-scale facilities, it is necessary to periodically monitor and timely identify defective areas, determine the necessary preventive measures and plan priority repairs. This is especially relevant in the military and post-war periods, when infrastructure facilities suffer significant damage.

Non-destructive testing (NDT) methods are widely used as a diagnostic tool for engineering structures to assess their technical condition [1–4]. Conventional NDT methods, such as ultrasonic testing [5, 6], magnetic particle method [7], acoustic emission [8, 9], infrared thermography [10, 11], etc., although showing a significant progress, have a number of limitations. In particular, their accuracy depends on external factors (humidity, temperature, noise level), and the interpretation of the results can be complicated by the subjective factor of the operator. In addition, such methods are labour-intensive, require high financial costs, and envisage direct personnel involvement, which increases the level of risks, especially when inspecting large-scale and hard-to-access structures.

One of the most effective ways to visually inspect engineering structures is to use unmanned ae-

rial vehicles (UAVs). Due to the rapid development of technologies, UAVs have been integrated into the system of remote monitoring of infrastructure facilities, demonstrating high efficiency in hard-to-access places where the use of traditional methods is limited [12–17]. Compared to traditional methods, surveys using UAVs are much faster and provide high spatial resolution of images. This allows obtaining detailed data with high accuracy, which is important for analyzing the condition of facilities and making reasoned decisions [18]. Their use not only improves the accuracy and speed of monitoring, but also significantly reduces the human and time resources, while minimizing the risks to the service personnel [19–22].

Due to the spread and improvement of artificial intelligence (AI) and neural networks (NN), the process of detecting defects in large-scale structures is gradually developing towards automation and intellectualization. This methodology is based on the high efficiency of neural networks in detecting and processing features, contributing to improving the quality and accuracy of the process of detecting defective areas.

The use of AI and NN in the field of data analysis is determined by their ability to automatically train and adapt to various input conditions, which makes these technologies promising in the context of improving the reliability and speed of defect localization processes on large-scale structural elements.

There are approaches to defect recognition based on the use of different NN architectures, training methods, and the choice of hyperparameters. The

NN hyperparameters are set manually or automatically before the training process starts: the number of layers in the NN, the type of activation function, the optimizer, etc. The choice of hyperparameters significantly affects the model accuracy, training speed, and quality of the obtained results. In particular, convolutional neural networks (CNNs) are quite effectively used to solve the problems of classification, segmentation, recognition and detection of defects in images.

With the development of computing capacities and the growth of image databases [23], CNN architectures continue to improve [24]. Compared to standard feed-forward NNs, convolutional NNs have significantly fewer couplings and parameters, which makes them less resource-intensive in training. CNNs use assumptions about the locality of pixel interactions, which allows them to effectively outline key structural elements of an image, reducing the number of parameters that need to be optimized [25].

Convolutional NNs are particularly effective for image processing tasks, as they automatically identify various image features at different levels of their representation. Due to applying the convolutional operation, CNNs are able to detect structural features in the input data, which ensures high accuracy in classification [26], segmentation [27, 28], and object recognition tasks [29, 30].

In recent years, the scientific community has made a significant progress in the application of machine training methods in various fields. In particular, NNs are actively used to detect defective areas based on images, including crack detection in concrete [31], exfoliation and surface delamination processes [32], fatigue cracks [33], and corrosion of steel structures [34]. The introduced image processing methods can partially replace the traditional monitoring carried out by operators in-situ, providing more efficient and accurate detecting features of defects on concrete and metal surfaces [35–38]. A considerable interest is paid to studies demonstrating the effectiveness of using UAVs in combination with deep training methods for the accurate identification of defective areas [39, 40].

Thus, the introduction of AI into the remote diagnostics of large-scale structures is a relevant area of automated diagnostics development aimed at enhancing the monitoring efficiency, optimizing resources, and improving the accuracy, speed, and reliability of detecting defective areas.

## METHODOLOGY. DATA COLLECTION AND PREPARATION FOR NEURAL NETWORK TRAINING

The Kyiv TV tower, which suffered structural damage as a result of a missile strike, was chosen as the

object of survey. A UAV with a camera resolution of  $5280 \times 3956$  pixels was used to conduct remote diagnostics of the lower tier of the Kyiv TV tower. Planning the flight path is an important step that directly affects the efficiency of remote monitoring and data collection tasks.

The overflight methodology involved the following stages:

- determining a flight path that provides an optimal inspection of the object, taking into account the requirements for spatial positioning accuracy;
- taking into account the influence of external factors, such as weather conditions (wind, angle of incidence of sunlight, precipitation), safety rules (altitude restrictions, restricted flight zones), accuracy requirements (resolution, coverage).

The remote monitoring of the lower tier of the Kyiv TV tower consisted of video scanning of the outer surface from bottom to top, trajectory correction by side movement, and further scanning in the opposite direction (top to bottom). Taking into account the geometric parameters and configuration of the elevator shaft, the flight was performed in a circular path. The closed flight path around the shaft minimizes the risk of loss of spatial coverage.

To minimize the impact of uneven lighting, the monitoring was carried out under stable weather conditions with an even distribution of natural light. This allowed avoiding sharp contrasts and improving image quality for further analytics.

An analysis of possible risks was conducted, which involved:

- alternative flight routes;
- backup takeoff and landing points;
- algorithms for emergency return of an UAV in case of loss of communication.

The data was collected at the lowest possible distance to the object in the “slow flight” mode, which helped to enhance the spatial resolution and quality of the obtained images. Optimization of the viewing angle was achieved by dynamically adjusting the camera tilt to minimize shadowing and ensure a full coverage of structural elements. The flight height was varied depending on the size of the structural elements of the lower tier of the TV tower to obtain highly detailed images from different angles.

After data collection, the images were processed, which involved the following steps:

- framing, which resulted in generating a set of images with a resolution of  $5472 \times 3078$  pixels;
- size adaptation for further processing by the neural network, namely, each image was divided into smaller fragments of  $128 \times 128$  pixels with an overlap of 50 % in width and height. This approach ensured a

uniform coverage of the images and the creation of a diverse training set. As a result, 14187 segments were obtained, that were prepared for NN training;

- annotating defective areas, which was carried out in the Labelme software environment using polygon meshes, which allowed for accurate marking the contours of objects by approximating with polygons;
- normalization of brightness and contrast in the Labelme software environment, which allowed for detection of low-contrast damage that was not clearly visible in the output images;
- classification of damage in the images into two types: corrosion and significant structural defects (holes, cracks);
- creation of masks that were used to segment the damage and outline the key areas of analysis.

## NEURAL NETWORK ARCHITECTURE

Detecting structural defects in images is a segmentation task that involves classifying each pixel of the input image. Convolutional neural networks (CNNs) are used to solve such tasks, in particular, the U-Net architecture and its modifications. Differences between the U-Net variations: number of layers and filters, use of normalization, type of activation function, loss function, etc. [41].

In order to improve the segmentation efficiency, a series of experiments were conducted with different configurations of the U-Net architecture (Figure 1). The following parameters varied: the initial number of convolutional layer filters, the number of convolutional operation levels, and the activation functions.

To improve the efficiency of the NNs based on the U-Net architecture, the following improvements were used:

- adding a concatenation mechanism for the corresponding encoder and decoder layers to preserve spatial information;
- doubling of the number of convolutional layers to improve the model's ability to extract features;
- normalizing input data to enhance the stability of the training process.

## NEURAL NETWORK TRAINING

The NN models were implemented in Python 3.10.12 using the TensorFlow and Keras libraries, version 2.9.0. During NN training, its parameters were saved after each training epoch.

The created dataset was divided into training, validation, and test sets in the ratio of 80 to 20 %. The training dataset (images with corresponding meshes) was used to train the model, taking into account the training parameters, such as the number of epochs, the batch size, the training speed, and the loss function. Additionally, optimizers were used to adapt the model weights to minimize the loss function during training and to ensure efficient training and model convergence.

Data augmentation was used to enhance the model's generalization capability, i.e. its ability to work correctly on new, previously unseen data. This is an artificial increase in the diversity of the training set that improves the model's stability. For images, augmentation involved such methods as rotation, colour change, etc.

The parameters were optimized using the Adam algorithm with the Sparse Categorical Crossentropy loss function, where Adam is an algorithm that helps the neural network in finding the optimal weights faster and more accurately during training. Sparse Categorical Crossentropy is a way to measure NN error in

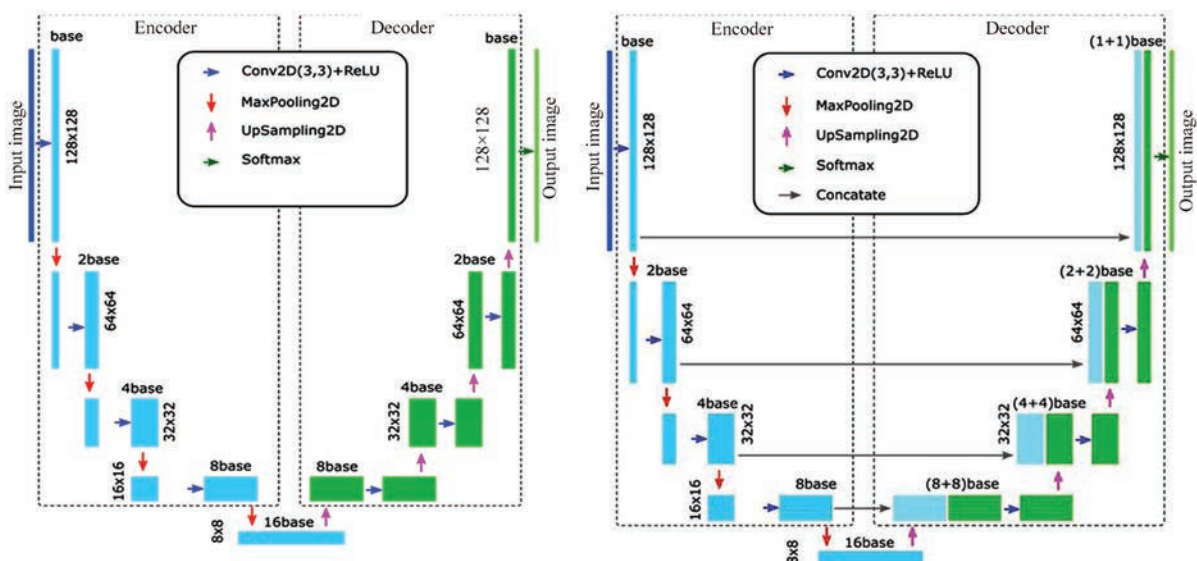


Figure 1. Architecture of the U-Net model: *a* — baseline model; *b* — model with additional layer coupling

**Table 1.** Influence of activation functions on U-Net model with different number of filters and parameters calculated during training

Initial number of filters (base)	Error on the training dataset (loss)	Error on the test dataset (val_loss)	Number of epochs	Number of model param- eters
Linear function for activating the last layer				
4	0.0907	0.1131	20/50	49267
8	0.0520	0.0874	33/50	196451
16	0.0761	0.0894	15/50	784579
Activation of the last Softmax layer				
4	0.0561	0.0758	43/50	49267
8	0.0486	0.0824	30/50	196451
16	0.0626	0.1012	16/50	784579

classification when each image or object belongs to one of several classes.

The influence of different activation functions in the last layer of the network, including linear and Softmax was also tested, which allowed evaluating their effectiveness in recognizing classes of defects (Table 1).

The Softmax function is an activation function that is often used in machine learning, especially in classification tasks with several classes [41]. It converts a vector of arbitrary numbers (output values of a neural network) into a probability vector, where each value corresponds to the probability of belonging to a certain class. For the vector  $z = [z_1, z_2, \dots, z_n]$ , where  $z_i$  is the output of the neural network for the  $i$ -th class, the Softmax function is calculated by the formula:

$$\text{Softmax}(z_i) = \frac{e^{z_i}}{\sum_{j=1}^n e^{z_j}}$$

where  $e^{z_i}$  is the exponent of the  $i$ -th element of the vector  $z$ ;  $\sum_{j=1}^n e^{z_j}$  is the sum of the exponents of all elements of the vector  $z$ .

Softmax is a probability vector where each value is in the range from zero to one, and the sum of all values is 1.

Table 1 shows the results of NN training, where the influence of the initial number of convolutional layer filters and the activation function of the output layer on the model accuracy is investigated. The evaluation is based on the loss function for the training (loss) and test (val\_loss) datasets, the number of epochs required for training, and the total number of model parameters.

Comparison of the two output layer options (linear activation and Softmax) shows that using Softmax provides a lower test error (val\_loss) in all configurations. This indicates a better generalization ability of the model, especially with fewer filters.

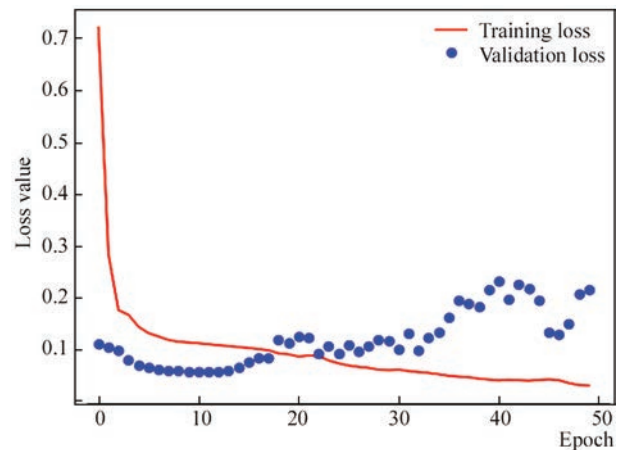
An increase in the number of filters (from 4 to 16) leads to an increase in the number of model parameters, which can improve its training ability, but also

increases the risk of overtraining, when the model demonstrates high accuracy on training data, losing the ability to generalize on new, previously unseen test or actual data, especially when using a large number of filters (base = 16). This is confirmed by an increase in the error on the test set (val\_loss) after 15–20 epochs of training, which indicates a possible transition from generalization to overtraining.

Figure 2 shows the dependence of the loss function for the training and test datasets on the number of epochs during NN training when using a model with a linear activation function and a base number of filters of 4 (base = 4).

In the initial stages of training (0–10 epochs), there is a rapid decrease in both errors (loss and val\_loss), which indicates that the model is training effectively. However, after the 20<sup>th</sup> epoch, the error on the training dataset (train\_loss) continues to decrease, while the error on the test dataset (val\_loss) starts to increase. This is a sign of overtraining, when the model loses its ability to generalize to new data. Thus, the optimal number of training iterations is 20 epochs, which prevents overmemorization of training samples.

One of the main characteristics that determine the effectiveness of NNs is the segmentation error (val\_loss) on images that were not used to train the CNN model. As a result of carried out research, it was


**Figure 2.** Dependence of the loss function for the training and validation datasets on the number of epochs during neural network training



**Table 2.** Testing results of improved U-Net models

Initial number of filters (base)	Error on the training dataset (loss)	Error on the test dataset (val_loss)	Number of epochs	Number of model param- eters
Baseline model + block coupling				
4	0.0683	0.0703	36/50	61507
8	0.0601	0.0599	18/50	245411
16	0.0314	0.0656	36/50	980419
Baseline model with a doubled number of convolutional layers + block coupling				
4	0.1335	0.1342	26/50	86107
8	0.0483	0.0841	21/50	343571
16	0.0658	0.0527	10/50	1372579
Baseline model with a doubled number of convolutional layers + block coupling + normalization				
4	0.0403	0.0518	48/50	86587
8	0.0292	0.0575	15/50	344531
16	0.0308	0.0598	14/50	1374499

found that the error of defect detection ranged from 7 to 11 % (Table 1).

The optimal model configuration for generalizing the results is to use eight filters together with the Softmax activation function. This configuration provides the lowest test error value (0.0824).

The results of testing various modifications of the U-Net architecture with varying the initial number of filters, the number of convolutional layers, using normalization, and increasing the number of blocks are shown in Table 2.

Three variants of the U-Net model architecture were studied:

- baseline model with additional block coupling;
- baseline model with a doubled number of convolutional layers with block coupling;
- baseline model with a doubled number of convolutional layers, block coupling and normalization.

Each of these architectures was tested with a different initial number of filters (base = 4, 8, 16), which resulted in 9 different model configurations.

The baseline model with an increased number of blocks shows improved results compared to the initial architecture, but its accuracy is limited, especially with a small number of filters. Adding additional con-

volutional layers reduces the error on the training set, but without normalization, instability is observed on the test data, which is especially noticeable with the initial number of filters, base = 4 (val\_loss = 0.1342). The use of normalization in combination with an increase in the number of blocks and convolutional layers allows achieving a minimum error value on the test set val\_loss = 0.0518 with base = 4, which indicates the effectiveness of this approach for less complex architectures. Thus, the best option is an architecture with a doubled number of convolutional layers, increased blocks, and normalization, which minimizes the error with a controlled model complexity.

Figure 3 shows the dependence of the loss function for the training and test datasets on the number of epochs during training of the baseline model with additional block coupling, as well as the improved U-Net model with a doubled number of convolutional layers, block coupling, and layer normalization.

The baseline model with additional block coupling (Figure 3, *a*) demonstrates fast training, but it is prone to overtraining, as evidenced by an increase in the error on the test dataset (val\_loss) after 20 epochs.

Compared to Figure 2, a significant decrease in the difference in error values during training to 3–5 % can

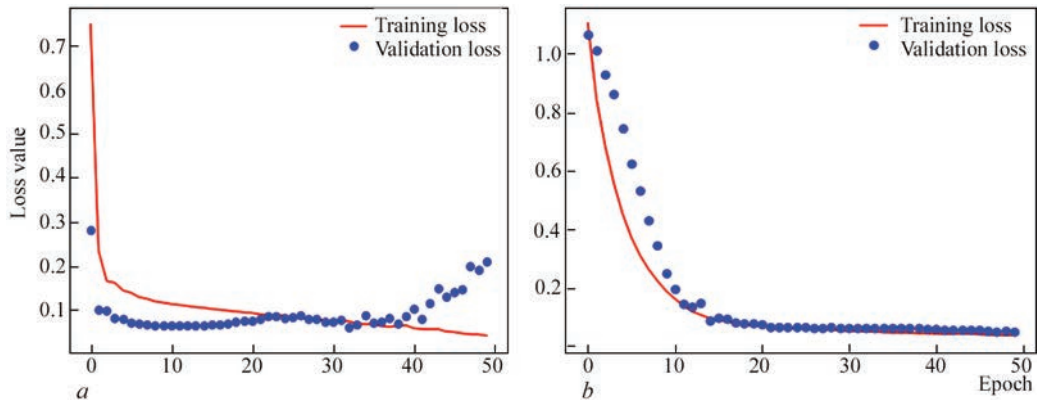


**Figure 3.** Dependence of the loss function for the training and test image datasets: *a* — baseline model with additional block coupling; *b* — improved U-Net model with a doubled number of convolutional layers, block coupling and layer normalization

be seen, which indicates a more accurate calculation of model parameters compared to using the baseline U-Net architecture (Figure 3, *a*).

At the initial stages of training (0–10 epochs) of the improved U-Net model (Figure 3, *b*), the values of the loss function for the training (loss) and test (val\_loss) sets decrease rapidly. The close values of these errors at the start are explained by the fact that the model has not yet formed complex patterns and generalizations, therefore its efficiency on training and test data is similar. In the course of further training, the model adapts to the peculiarities of the training data. After 15–20 epochs, the training and test errors stabilize without significant differences, indicating good generalization and lack of overtraining. This indicates that the model has achieved optimal efficiency and can be effectively generalized to new data. Thus, the proposed modifications to the U-Net architecture have improved the model's accuracy in detecting defects in images of structures.

ANALYSIS OF THE OBTAINED RESULTS

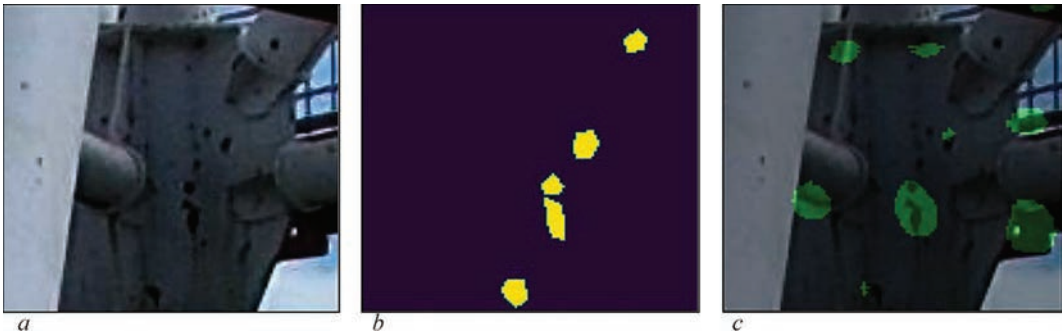
Figure 4 shows the results of automatic detection of damaged areas in the images using the baseline model with the number of filters base = 4. A visual comparison of the areas marked by the operator (Figure 4, *b*) and the segmented areas obtained by the neural

network (Figure 4, *c*) shows that the model is able to detect damage that remained unnoticed by the operator. However, the segmentation result obtained by the neural network has a significant error, missing areas, which indicates insufficient accuracy.

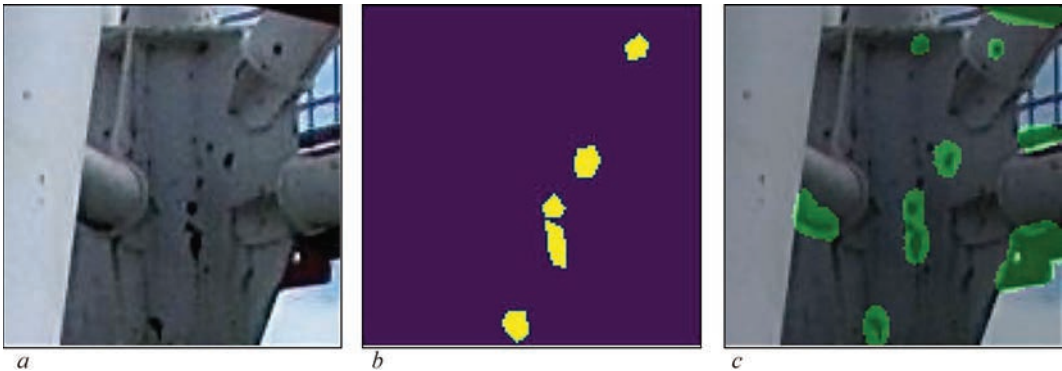
Figure 5 shows the results of applying the improved U-Net model, the number of filters base = 16 and with Softmax activation, which show a more accurate segmentation of defective areas, reducing the number of false classifications compared to the baseline version (Figure 4).

Figure 6 shows an example where the NN successfully identified a defective area caused by the penetration of debris through the wall of a tubular element of the TV tower, which was missed by the operator when creating the annotation. Comparison of the masks (Figures 6, *b* and 6, *c*) shows that the predicted damage areas coincide well with the actual data. This confirms the effectiveness of the model. The obtained results confirm the model's ability to detect damage that may remain unnoticed, thereby minimizing the influence of the human factor during the visual diagnostics of structures.

The obtained results demonstrate the effectiveness of the U-Net neural network for automatic damage detection. However, incomplete or inaccurate marking of defective areas by the operator in the training



**Figure 4.** Automatic detection of damaged areas by the model with parameters: base = 4, the last activation layer is linear: *a* — fragment of the image with the damaged assembly; *b* — damaged areas marked by the operator in yellow; *c* — result of segmentation obtained by the neural network (green)



**Figure 5.** Automatic detection of damaged areas using the improved U-Net model with parameters: base = 16, the last activation layer is Softmax: *a* — fragment of the image with the damaged assembly; *b* — damaged areas marked by the operator in yellow; *c* — result of segmentation obtained by the neural network (green)

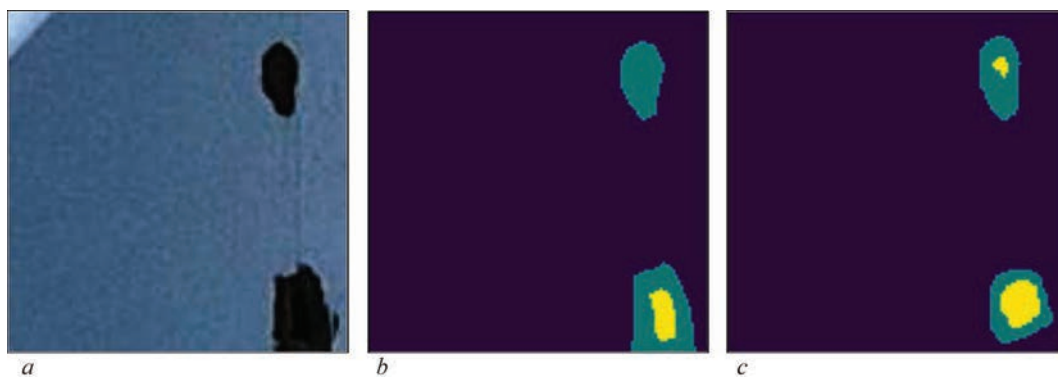


**Figure 6.** Automatic detection of damaged areas using the improved U-Net model with parameters: base = 16, the last activation layer is Softmax: *a* — fragment of the image with damaged areas; *b* — damaged areas marked by the operator; *c* — result of segmentation obtained by the neural network. Green colour indicates a corrosion damage, yellow — a hole. Model, number of filters — 16 (base = 16) with the last activation Softmax layer

dataset can negatively affect the quality of the model, since its training depends on the correspondence to the meshes marked by the operator. Therefore, the formation of a high-quality database with complete and accurate defect marking is an important factor in creating a highly accurate NN.

## CONCLUSIONS

The carried out study confirmed the effectiveness of using neural networks for automated defect detection, which helps to improve the diagnostic accuracy and minimize the influence of the subjective factor.

The analysis of the effectiveness of different neural network architectures showed that models with more filters provide an improved defect detection capability, but their use requires significant computing resources and training time. The modified U-Net architectures, in particular by adding additional blocks and normalization, allowed reducing the defect detection error to 3–5 %, which is a significant improvement over the baseline models. It was found that the optimal number of iterations for training models with a modified architecture is 15–20, since further training leads to overtraining and an increase in the error on test data.

The use of modified neural network architectures with the use of mechanisms for normalization and adaptive adjustment of hyperparameters is a promising direction for improving the accuracy and reliability of automated defect diagnostics based on image analysis, which opens up opportunities for further integration of such systems into the monitoring process.

## ACKNOWLEDGMENTS

The published results were obtained within the framework of the project 022.01/0095 “Development of technology for remote diagnostics of damaged large-scale objects based on the use of unmanned aerial vehicles (UAVs) and photogrammetry” funded by the National Research Foundation of Ukraine in the

framework “Science for the Recovery of Ukraine in the War and Post-War Periods”.

## REFERENCES

1. Balayssac, J.-P., Garnier, V. et al. (2018) *Non-Destructive testing and evaluation of civil engineering structures*. STE Press Ltd., Elsevier Science. DOI: <https://doi.org/10.1016/C2016-0-01227-5>
2. Reddy, K.A. (2017) Non-destructive testing, evaluation of stainless steel materials. *Mater. Today Proc.*, **4**(8), 7302–7312. DOI: <https://doi.org/10.1016/j.matpr.2017.07.060>
3. Deepak, J.R., Raja, V.K.B., Srikanth, D. et al. (2021) Non-destructive testing (NDT) techniques for low carbon steel welded joints: A review and experimental study. *Mater. Today Proc.*, **44**(8), 3732–3737. DOI: <https://doi.org/10.1016/j.matpr.2020.11.578>
4. Polimeno, M., Roselli, I., Luprano, V.A.M. et al. (2018) A non-destructive testing methodology for damage assessment of reinforced concrete buildings after seismic events. *Eng. Structures*, **163**, 122–136. DOI: <https://doi.org/10.1016/j.engstruct.2018.02.053>
5. Bahunar, M., Safizadeh, M. (2021) Investigation of real delamination detection in composite structure using air-coupled ultrasonic testing. *Composite Structures*, **280**, 114939. DOI: <https://doi.org/10.1016/j.compstruct.2021.114939>
6. Chen, Y., Kang, Y., Feng, B., Li, Y., Cai, X. (2022) Automatic defect identification in magnetic particle testing using a digital model aided de-noising method. *Measurement*, **198**, 111427. DOI: <https://doi.org/10.1016/j.measurement.2022.111427>
7. Van Steen, C., Pahlavan, P., Wevers, M., Verstrynghe, E. (2018) Localisation and characterisation of corrosion damage in reinforced concrete by means of acoustic emission and X-ray computed tomography. *Construction and Building Materials*, **197**, 21–29. DOI: <https://doi.org/10.1016/j.conbuildmat.2018.11.159>
8. Suzuki, T., Ogata, H., Takada, R. et al. (2010) Use of acoustic emission and X-ray computed tomography for damage evaluation of freeze-thawed concrete. *Construction and Building Materials*, **24**, 2347–2352. DOI: <https://doi.org/10.1016/j.conbuildmat.2010.05.005>
9. Pedram, M., Taylor, S., Hamill, G. et al. (2022) Experimental evaluation of heat transition mechanism in concrete with subsurface defects using infrared thermography. *Construction and Building Materials*, **360**, 129531. DOI: <https://doi.org/10.1016/j.conbuildmat.2022.129531>
10. Shrestha, P., Avcı, O., Rifai, S. et al. (2025) A review of infrared thermography applications for civil infrastructure. *Struc-*



- tural Durability & Health Monitoring*, 19(2), 193–231. DOI: <https://doi.org/10.32604/sdhm.2024.049530>
11. Lobanov, L.M., Stelmakh, D., Shkurat, I. et al. (2025) Determination of a TV tower verticality using UAVs, RTK and photogrammetry. In: *Proc. of VII<sup>th</sup> Inter. Conf. on Welding and Related Technologies, Yaremche, Ukraine, 7–10 October 2024*, 149–153. DOI: <https://doi.org/10.1201/9781003518518-30>
12. Lobanov, L., Stelmakh, D., Savitsky, V. et al. (2024) Damage detection and analysis using unmanned aerial vehicles (UAVs) and photogrammetry method. *Procedia Structural Integrity*, 59, 43–49. DOI: <https://doi.org/10.1016/j.prostr.2024.04.008>
13. Lobanov, L.M., Stelmakh, D.I., Savitsky, V.V. et al. (2023) Remote assessment of damage to Kyiv TV tower based on the application of aerial photography and photogrammetry method. *Tekh. Diagnost. ta Neruiniv. Kontrol*, 3, 16–20 [in Ukrainian]. DOI: <https://doi.org/10.37434/tdnk2023.03.03>
14. Onososen, A., Musonda, I., Onatayo, D. et al. (2023) Impediments to construction site digitalization using unmanned aerial vehicles (UAVs). *Drones*, 7(1), 45. DOI: <https://doi.org/10.3390/drones7010045>
15. Albeaino, G., Gheisari, M., Franz, B.W. (2019) A systematic review of unmanned aerial vehicle application areas and technologies in the AEC domain. *J. of Information Technology in Construction*, 24, 381–405. DOI: <https://doi.org/www.itcon.org/2019/20>
16. Ham, Y., Han, K.K., Lin, J.J., Golparvar-Fard, M. (2016) Visual monitoring of civil infrastructure systems via camera-equipped unmanned aerial vehicles (UAVs): A review of related works. *Visualization in Eng.*, 4, 1. DOI: <https://doi.org/10.1186/s40327-015-0029-z>
17. Pant, S., Nooralishahi, P., Avdelidis, N.P. et al. (2021) Evaluation and selection of video stabilization techniques for UAV-based active infrared thermography application. *Sensors*, 21, 1604. DOI: <https://doi.org/10.3390/s21051604>
18. Ciampa, E., De Vito, L., Rosaria Pecce, M. (2019) Practical issues on the use of drones for construction inspections. *J. of Physics: Conf. Series*, 1249, 012016. DOI: <https://doi.org/10.1088/1742-6596/1249/1/012016>
19. Duque, L., Seo, J., Wacker, J. (2018) Synthesis of unmanned aerial vehicle applications for infrastructures. *J. Perform. Constr. Facil.*, 32(4). DOI: [https://doi.org/10.1061/\(ASCE\)CF.1943-5509.0001185](https://doi.org/10.1061/(ASCE)CF.1943-5509.0001185)
20. Rakha, T., Gorodetsky, A. (2018) A review of unmanned aerial system (UAS) applications in the built environment: Towards automated building inspection procedures using drones. *Aut. in Constr.*, 93, 252–264. DOI: <https://doi.org/10.1016/j.autcon.2018.05.002>
21. Wu, W., Qurishee, M.A., Owino, J. et al. (2018) Coupling deep learning and UAV for infrastructure condition assessment automation. In: *Proc. of IEEE Inter. Smart Cities Conf., ISC2, 2018 Sept. 16–19, Kansas City, MO, USA*. DOI: <https://doi.org/10.1109/ISC2.2018.8656971>
22. Gu, J., Wang, Z., Kuen, J. et al. (2016) Recent advances in convolutional neural networks. *Pattern Recognition*, 77, 354–377. DOI: <https://doi.org/10.1016/j.patcog.2017.10.013>
23. Gulgec, N.S., Takáč, M., Pakzad, S.N. (2017) Structural damage detection using convolutional neural networks. In: *Proc. of Conf. on Society for Experimental Mechanics Series*, 331–337. DOI: [https://doi.org/10.1007/978-3-319-54858-6\\_33](https://doi.org/10.1007/978-3-319-54858-6_33)
24. Krizhevsky, A., Sutskever, I., Hinton, G. (2012) Imagenet classification with deep convolutional neural networks. *Advances in Neural Information Processing Systems*, 25(2), 1097–1105. DOI: <https://doi.org/10.1145/3065386>
25. Lee, S.Y., Tama, B.A., Moon, S.J., Lee, S. (2019) Steel surface defect diagnostics using deep convolutional neural network and class activation map. *Applied Sci.*, 9(24), 5449. DOI: <https://doi.org/10.3390/app9245449>
26. Tabernik, D., Šela, S., Skvarc, J., Skocaj, D. (2020) Segmentation-based deep-learning approach for surface-defect detection. *J. of Intelligent Manufacturing*, 31(3), 759–776. DOI: <https://doi.org/10.1007/s10845-019-01476-x>
27. Prappacher, N., Bullmann, M., Bohn, G. et al. (2020) Defect detection on rolling element surface scans using neural image segmentation. *Applied Sci.*, 10(9), 3290. DOI: <https://doi.org/10.3390/app10093290>
28. Li, J., Su, Z., Geng, J., Yin, Y. (2018) Real-time detection of steel strip surface defects based on improved YOLO detection network. *IFAC-PapersOnLine*, 51(21), 76–81. DOI: <https://doi.org/10.1016/j.ifacol.2018.09.412>
29. Wei, R., Song, Y., Zhang, Y. (2020) Enhanced faster region convolutional neural networks for steel surface defect detection. *ISIJ Inter.*, 60(3), 539–545. DOI: <https://doi.org/10.2355/isijinternational.isijint-2019-335>
30. Cha, Y.-J., Choi, W., Buyukozturk, O. (2017) Deep learning-based crack damage detection using convolutional neural networks. *Computer-Aided Civil and Infrastructure Eng.*, 32(5), 361–378. DOI: <https://doi.org/10.1111/mice.12263>
31. Hutchinson, T., Chen, Z. (2006) Improved image analysis for evaluating concrete damage. *J. of Computing in Civil Eng.*, 20(3), 210–216. DOI: [https://doi.org/10.1061/\(ASCE\)0887-3801\(2006\)20:3\(210\)](https://doi.org/10.1061/(ASCE)0887-3801(2006)20:3(210))
32. Dung, C., Sekiya, H., Hirano, S. et al. (2019) A vision-based method for crack detection in gusset plate welded joints of steel bridges using deep convolutional neural networks. *Automation in Construction*, 102, 217–229. DOI: <https://doi.org/10.1016/j.autcon.2019.02.013>
33. Shen, H.-K., Chen, P.-H., Chang, L.-M. (2013) Automated steel bridge coating rust defect recognition method based on color and texture feature. *Automation in Construction*, 31, 338–356. DOI: <https://doi.org/10.1016/j.autcon.2012.11.003>
34. Xu, Y., Bao, Y., Chen, J. et al. (2018) Surface fatigue crack identification in steel box girder of bridges by a deep fusion convolutional neural network based on consumer-grade camera images. *Structural Health Monitoring*, 18(3), 653–674. DOI: <https://doi.org/10.1177/1475921718764873>
35. Prasanna, P., Dana, K.J., Gucunski, N. et al. (2016) Automated crack detection on concrete bridges. *IEEE Transact. on Automation Sci. and Eng.*, 13(2), 591–599. DOI: <https://doi.org/10.1109/TASE.2014.2354314>
36. An, Y.-K., Jang, K.-Y., Kim, B., Cho, S. (2018) Deep learning-based concrete crack detection using hybrid images. In: *Proc. of SPIE 10598 on Sensors and Smart Structures Technologies for Civil, Mechanical, and Aerospace Systems*, 1059812. DOI: <https://doi.org/10.1117/12.2294959>
37. Chow, J.K., Su, Z., Wu, J. et al. (2020) Anomaly detection of defects on concrete structures with the convolutional autoencoder. *Advanced Eng. Informatics*, 45, 101105. DOI: <https://doi.org/10.1016/j.aei.2020.101105>
38. Miranda, J., Veith, J., Larniere, S. et al. (2019) Machine learning approaches for defect classification on aircraft fuselage images acquired by an UAV. In: *Proc. of Fourteenth Inter. Conf. on Quality Control by Artificial Vision*, 1117208. DOI: <https://doi.org/10.1117/12.2520567>
39. Avdelidis, N.P., Tsourdos, A., Lafiosca, P. et al. (2022) Defects recognition algorithm development from visual UAV inspections. *Sensors*, 22(13), 4682. DOI: <https://doi.org/10.3390/s22134682>
40. Ronneberger, O., Fischer, P., Brox, T. (2015) U-net: convolutional networks for biomedical image segmentation. In: *Proc. of the Medical Image Computing and Computer-Assisted In-*



tervention, 234–241. <http://lmb.informatik.uni-freiburg.de/people/ronneber/u-net>

41. Ren, J., Wang, H. (2023) Calculus and optimization. In: *Mathematical Methods in Data Science*. Chapter 3. Elsevier, 51–89. DOI: <https://doi.org/10.1016/B978-0-44-318679-0.00009-0>

ORCID

L.M. Lobanov: 0000-0001-9296-2335,  
I.L. Shkurat: 0009-0003-1888-4203,  
D.I. Stelmakh: 0000-0002-0412-9747,  
O.P. Shutkevych: 0000-0001-5758-2396,  
V.V. Savitsky: 0000-0002-2615-1793

CONFLICT OF INTEREST

The Authors declare no conflict of interest

CORRESPONDING AUTHOR

I.L. Shkurat  
E.O. Paton Electric Welding Institute of the NASU  
11 Kazymyr Malevych Str., 03150, Kyiv, Ukraine.  
E-mail: [innashkurat2909@gmail.com](mailto:innashkurat2909@gmail.com)

SUGGESTED CITATION

L.M. Lobanov, I.L. Shkurat, D.I. Stelmakh,  
O.P. Shutkevych, V.V. Savitsky (2025) Enhancing  
large-scale structure diagnostics through UAV-based  
data and neural network analysis. *The Paton Welding  
J.*, 7, 28–36.  
DOI: <https://doi.org/10.37434/tpwj2025.07.05>

JOURNAL HOME PAGE

<https://patonpublishinghouse.com/eng/journals/tpwj>

Received: 06.03.2024

Received in revised form: 08.05.2024

Accepted: 26.06.2025



Developed at PWI

EQUIPMENT FOR ELECTRON BEAM WELDING

EBW mashines with small vacuum chambers (<10 m³)



**CB 112 mashine:** 0.3 m³, 60 kV, up to 15 kW

Large-sized EBW mashines  
with vacuum chambers >50 m³



**KL 118 mashine**

Medium-sized EBW mashines  
with vacuum chambers 10–50 m³



**KL 115 mashine:**  
36 m³, 60 kV, up to 60 kW



Aviation Titanium Profiles